Journal of Power Sources 220 (2012) 10–14

Contents lists available at SciVerse ScienceDirect

Journal of Power Sources

journal homepage: www.elsevier.com/locate/jpowsour

Short communication

Nonhumidified fuel cell using *N*-ethyl-*N*-methylpyrrolidinium fluorohydrogenate ionic liquid–polymer composite membranes

Pisit Kiatkittikul, Toshiyuki Nohira*, Rika Hagiwara*

Department of Fundamental Energy Science, Graduate School of Energy Science, Kyoto University, Sakyo-ku, Kyoto 606-8501, Japan

HIGHLIGHTS

- ► Composite membranes of EMPyr$(FH)_{1.7}F$ ionic liquid and HEMA polymer were prepared.
- ► They are thermally stable up to 423 K.
- ► Ionic conductivities are very high compared with other IL-based membranes.
- ► Power density of 32 mW cm^{-2} was observed at 323 K under nonhumidified condition.
- ► Performance deterioration from 353 K was explained by block of gas channel in GDEs.

ARTICLE INFO

Article history:
Received 7 July 2012
Accepted 31 July 2012
Available online 9 August 2012

Keywords:
Ionic liquid
Fluorohydrogenate anion
N-Ethyl-*N*-methylpyrrolidinium cation
Polymer composite membrane
Nonhumidified fuel cell

ABSTRACT

Composite membranes consisting of EMPyr$(FH)_{1.7}F$ (EMPyr = *N*-ethyl-*N*-methylpyrrolidinium) ionic liquid and hydroxyethylmethacrylate (HEMA) polymer (EMPyr$(FH)_{1.7}F$/HEMA monomer = 7:3, 8:2, and 9:1 in molar ratios) were prepared as electrolytes for a nonhumidified fuel cell. The composite membranes showed good thermal stability up to 453 K, regardless of the HEMA content. For the EMPyr$(FH)_{1.7}F$–HEMA (9:1) composite membrane, ionic conductivities were 8.9 and 81.9 mS cm^{-1} at 293 K and 373 K, respectively. In the single cell tests, a maximum power density of 32 mW cm^{-2} was observed at 323 K for a cell using the EMPyr$(FH)_{1.7}F$–HEMA (9:1) composite membrane under nonhumidified conditions.

1. Introduction

Polymer electrolyte fuel cells (PEFCs) are widely recognized as a promising power-generation device for future generations due to their major advantages such as high energy output, low emissions, and applicability to a wide range of applications [1–3]. However, conventional PEFCs using a Nafion® membrane require sufficient humidity for ionic conduction [4–7]. This restricts the operating temperature to temperatures below 373 K and requires a complicated humidification system. Thus, as a solution to these major drawbacks, a new membrane electrolyte that enables operation at elevated temperatures without humidification is required. Many types of proton-conducting materials have been developed as alternative membrane electrolytes, such as modified perfluorosulfonic acid (PFSA) polymer membranes [8–10], sulfonated hydrocarbon polymer membranes [8,11–13], acid–base complex membranes [14–16], polybenzimidazole (PBI)-based polymer membranes [16–20], and ionic liquid-based polymer membranes [21–27].

Room-temperature ionic liquids (RTILs) have recently attracted considerable attention because of their application to electrochemical devices and reaction media, due to notable properties such as high chemical and thermal stabilities, nonflammability, nonvolatility, and a wide electrochemical window [28–31]. Among various types of ionic liquids, fluorohydrogenate ionic liquids (FHILs), which consist of organic cations and fluorohydrogenate anions ($(FH)_nF^-$; n represents the average composition of HF in the anion), possess remarkable properties such as high ionic conductivity and a wide liquid-phase temperature range [31]. In recent years, we have studied and reported on a series of FHILs [32–40]. One of them, 1-ethyl-3-methylimidazolium fluorohydrogenate, EMIm$(FH)_nF$ (n = 1.3 and 2.3), was studied as an electrolyte for a nonhumidified fuel cell [41,42]. The presence of fluorohydrogenate anions $(FH)F^-$ and $(FH)_2F^-$ in EMIm$(FH)_{1.3}F$ and $(FH)_2F^-$ and $(FH)_3F^-$ in EMIm$(FH)_{2.3}F$, was identified by infrared spectroscopy [34].

* Corresponding authors. Tel.: +81 75 753 5822; fax: +81 75 753 5906.
E-mail addresses: nohira@energy.kyoto-u.ac.jp (T. Nohira), hagiwara@energy.kyoto-u.ac.jp (R. Hagiwara).

0378-7753/$ – see front matter © 2012 Elsevier B.V. All rights reserved.
http://dx.doi.org/10.1016/j.jpowsour.2012.07.124

Owing to a unique hydrogen and charge transportation mechanism via the fluorohydrogenate anions, $(FH)_nF^-$, water is not required for fuel cell operation. The anode, cathode, and total reactions for the fuel cell using $EMIm(FH)_{2.3}F$ as an electrolyte are expressed as follows [41,42]:

$$\text{Anode: } H_2 + 8(FH)_2F^- \rightarrow 6(FH)_3F^- + 2e^- \quad (1)$$

$$\text{Cathode: } 1/2O_2 + 6(FH)_3F^- + 2e^- \rightarrow 8(FH)_2F^- + H_2O \quad (2)$$

$$\text{Total: } H_2 + 1/2O_2 \rightarrow H_2O \quad (3)$$

where the $(FH)_2F^-$ and $(FH)_3F^-$ anions are involved in the reactions.

Hence, this type of fuel cell, denoted as a fluorohydrogenate fuel cell (FHFC), can be operated under nonhumidified conditions at an elevated temperature of 393 K.

In our recent studies, *N*-ethyl-*N*-methylpyrrolidinium fluorohydrogenate, $EMPyr(FH)_{1.7}F$, whose structure is shown in Fig. 1, was found to exhibit higher activity for the oxygen reduction reaction (ORR) on a Pt electrode [43]. It was also revealed that $EMPyr(FH)_{1.7}F$ possesses adequate oxygen permeability, with a crossover current as low as 0.143 mA cm^{-2} in the case of electrolyte thickness of 177.8 μm [44].

In this work, composite membranes of $EMPyr(FH)_{1.7}F$ and 2-hydroxyethylmethacrylate (HEMA) polymer were prepared to investigate their thermal and electrochemical properties. Then, using the composite membrane, the single-cell performance was studied under nonhumidified conditions. It should be noted that the anode, cathode, and total reactions for the FHFC in this study (using $EMPyr(FH)_{1.7}F$ as the electrolyte) are expressed as follows:

$$\text{Anode: } H_2 + 6(FH)F^- \rightarrow 4(FH)_2F^- + 2e^- \quad (4)$$

$$\text{Cathode: } 1/2O_2 + 4(FH)_2F^- + 2e^- \rightarrow 6(FH)F^- + H_2O \quad (5)$$

$$\text{Total: } H_2 + 1/2O_2 \rightarrow H_2O \quad (6)$$

where $(FH)F^-$ and $(FH)_2F^-$ anions are involved in the reactions.

2. Experimental

2.1. Preparation of $EMPyr(FH)_{1.7}F$–HEMA composite membranes

$EMPyr(FH)_{2.3}F$ was prepared using the method reported previously [34]. To prepare $EMPyr(FH)_{1.7}F$, which has a negligible vapor pressure up to 393 K, $EMPyr(FH)_{2.3}F$ was evacuated using a rotary pump through a chemical trap for four days and then directly through a cold trap for two days at 393 K under reduced pressure (<1 Pa). The *n* value of 1.7 was confirmed by elemental analysis of hydrogen, carbon, nitrogen, and fluorine using a CHN coder and a fluoride ion-selective electrode.

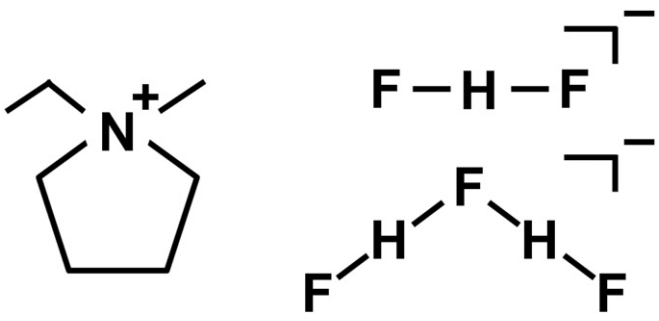

Fig. 1. Structures of $EMPyr^+$ cation, and $(FH)F^-$ and $(FH)_2F^-$ anions.

The mixed solutions of $EMPyr(FH)_{1.7}F$ and the HEMA monomer (Wako) were prepared in the molar ratios of 7:3, 8:2, and 9:1 under an argon atmosphere. A small amount (1 mol% of HEMA) of azobisisobutyronitrile (AIBN, Wako) was added as a radical initiator. Membrane filters (Omnipore™, Millipore, thickness: 65 μm, average pore diameter: 0.45 μm, porosity: 80%), which were used as porous supporting materials, were immersed in the mixtures. Each membrane filter was sandwiched between two PTFE sheets and then polymerized in a vacuum oven filled with argon gas at 343 K for 12 h.

2.2. Characterizations of $EMPyr(FH)_{1.7}F$–HEMA composite membranes

A differential thermogravimetric analyzer (DTG-60/60H, Shimadzu) was used to investigate the thermal stability of the $EMPyr(FH)_{1.7}F$ ionic liquid and the composite membranes from 323 K to 873 K at a scanning rate of 1 K min^{-1} under nitrogen atmosphere. Phase-transition behavior was examined by means of a differential scanning calorimeter (DSC-60, Shimadzu) between 123 K and 423 K at a scanning rate of 10 K min^{-1} under nitrogen atmosphere. To measure the ionic conductivity of the $EMPyr(FH)_{1.7}F$ ionic liquid, a T-shaped cell with two Pt rods at a fixed distance was used. The cell constant was determined using a 0.1 M KCl standard solution. To measure the ionic conductivity of the composite membranes, the four-point probe method was used. The measurement was carried out by the ac impedance method using a Solartron 1286 electrochemical interface combined with a Solartron 1260 frequency response analyzer (AMETEK) from 233 K to 393 K under nitrogen atmosphere.

2.3. Fabrication of membrane–electrode assembly and single cell test

The membrane–electrode assembly (MEA) was prepared by placing the composite membrane between two gas diffusion electrodes (GDEs, 1.0 mg Pt cm^{-2}, ionomer-free, KM Lab) with a geometric surface area of 5 cm^2. After fabricating the composite membrane into a single cell with fuel-cell hardware (EFC-05-02-H2R, 5 cm^2, ElectroChem), the single cell test was performed using a Solartron 1286 electrochemical interface in a temperature-controlled chamber (Espec) from 298 K to 393 K under nonhumidified conditions. Anhydrous H_2 (99.999%) was supplied from a hydrogen generator (HORIBA STEC) and O_2 was supplied from a cylinder (99.9999%). The gas flow rates of H_2 and O_2 were 20 mL min^{-1}.

2.4. Cross-sectional SEM observation

The samples of MEAs before and after the single cell test were cross-sectioned by a knife and embedded with resin into a block. The sample block was then polished with emery paper to expose the cross section. The surface was coated with Au by ion-sputtering (E-1010, Hitachi) prior to observation by scanning electron microscope (SEM, VE-8800, Keyence).

3. Results and discussion

3.1. Thermogravimetric and differential scanning calorimetry analysis

Fig. 2 shows TGA curves for the $EMPyr(FH)_{1.7}F$ ionic liquid and the $EMPyr(FH)_{1.7}F$–HEMA (9:1, 8:2, and 7:3 in molar ratio) composite membranes. For $EMPyr(FH)_{1.7}F$, decomposition is observed from approximately 453 K. In the case of the

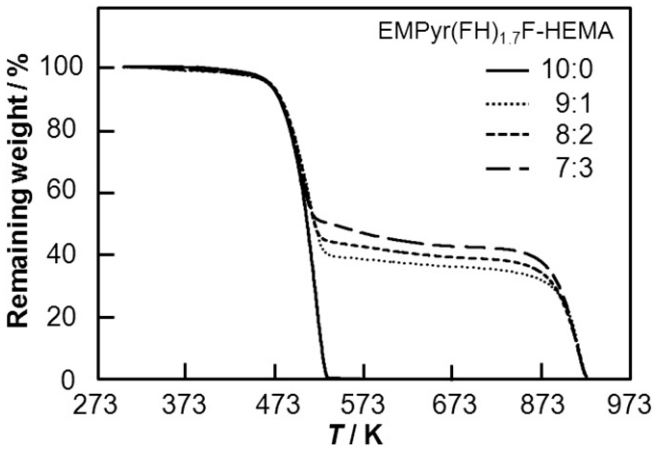

Fig. 2. TG curves for $EMPyr(FH)_{1.7}F$ ionic liquid (10:0) and $EMPyr(FH)_{1.7}F$–HEMA composite membranes (9:1, 8:2, and 7:3).

$EMPyr(FH)_{1.7}F$–HEMA composite membranes, the initial weight loss also starts at 453 K. The value of the initial weight loss cannot be explained only by the decomposition of $EMPyr(FH)_{1.7}F$ because decomposition of HEMA also occurs. These two decompositions are indistinguishable because they proceed in almost the same temperature range. The final weight loss at 753 K corresponds to the decomposition of the membrane (PTFE) filter. These results indicate that the composite membranes are thermally stable up to 453 K, regardless of HEMA content.

Phase-transition behaviors were investigated by means of DSC, as shown in Fig. 3. The melting point was found to be 253 K for the $EMPyr(FH)_{1.7}F$ ionic liquid and 203 K for the $EMPyr(FH)_{1.7}F$–HEMA (9:1) composite membrane. However, a melting point was not observed for the $EMPyr(FH)_{1.7}F$–HEMA (8:2) composite membrane. The decrease in the melting point suggests an interaction between the $EMPyr(FH)_{1.7}F$ ionic liquid and the HEMA polymer. As expected, the interaction becomes stronger with an increase in the HEMA content.

3.2. Ionic conductivities

The ionic conductivities were measured from 233 K to 393 K under nonhumidified conditions. Fig. 4 shows Arrhenius plots of

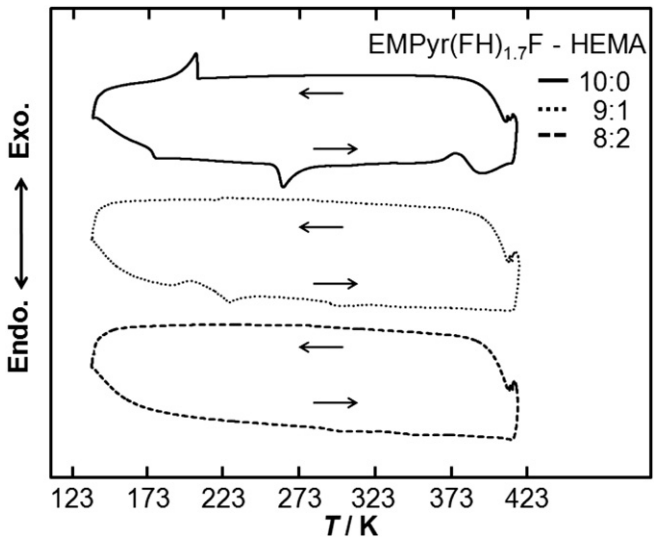

Fig. 3. DSC results for $EMPyr(FH)_{1.7}F$ ionic liquid (10:0) and $EMPyr(FH)_{1.7}F$–HEMA composite membranes (9:1 and 8:2).

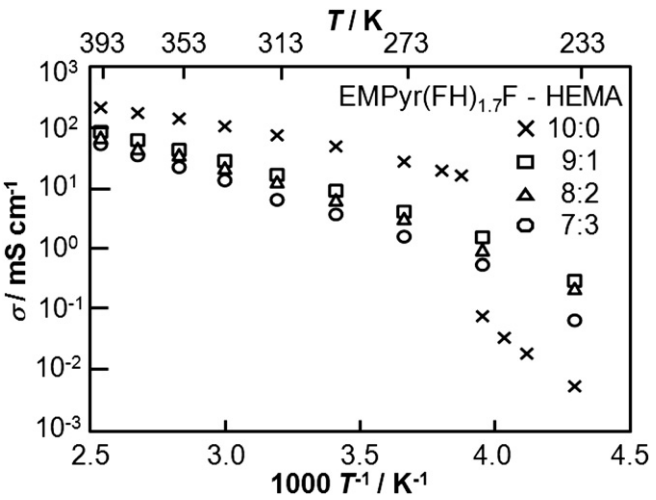

Fig. 4. Arrhenius plots of ionic conductivities for $EMPyr(FH)_{1.7}F$ ionic liquid (10:0) and $EMPyr(FH)_{1.7}F$–HEMA composite membranes (9:1, 8:2, and 7:3).

ionic conductivities for the $EMPyr(FH)_{1.7}F$ ionic liquid and the $EMPyr(FH)_{1.7}F$–HEMA (9:1, 8:2, and 7:3) composite membranes. The ionic conductivity increases with an increase in the FHIL content. For the $EMPyr(FH)_{1.7}F$ ionic liquid, the ionic conductivities were 46.7 and 204.7 mS cm^{-1} at 293 K and 393 K, respectively. A sudden drop in the ionic conductivity occurred at 253 K, which is explained by the solidification of the $EMPyr(FH)_{1.7}F$ ionic liquid, whose melting point is 253 K. However, this drop was not observed in any of the $EMPyr(FH)_{1.7}F$–HEMA composite membranes, whose melting points are significantly below the measuring range of ionic conductivity. For the $EMPyr(FH)_{1.7}F$–HEMA (9:1) composite membrane, the ionic conductivities were 8.7 and 81.9 mS cm^{-1} at 298 K and 393 K, respectively. These values are very high compared with previously reported values for composite membranes using similar FHILs [42] and other ionic liquid-based polymer membranes [21–27].

3.3. Single cell test under nonhumidified conditions

A single cell using the $EMPyr(FH)_{1.7}F$–HEMA (9:1) composite membrane was operated at 298, 323, 353, and 393 K under non-humidified condition. Fig. 5 shows the current density–voltage (i–v) and current density–power density (i–p) curves. From

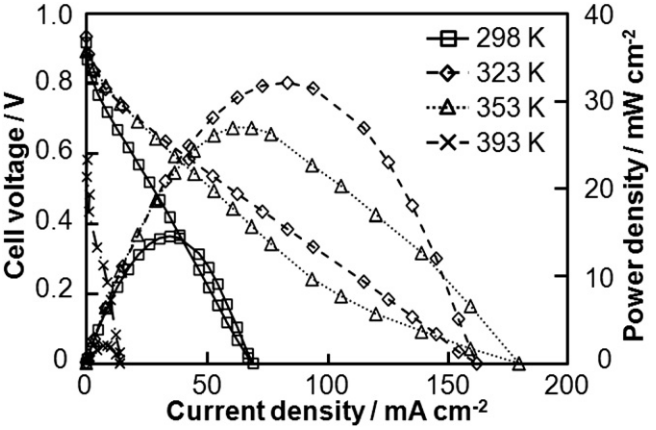

Fig. 5. i–V and i–p curves of a single cell using $EMPyr(FH)_{1.7}F$–HEMA (9:1) composite membrane under nonhumidified conditions. Anode and cathode catalyst: 1.0 mg Pt cm^{-2}.

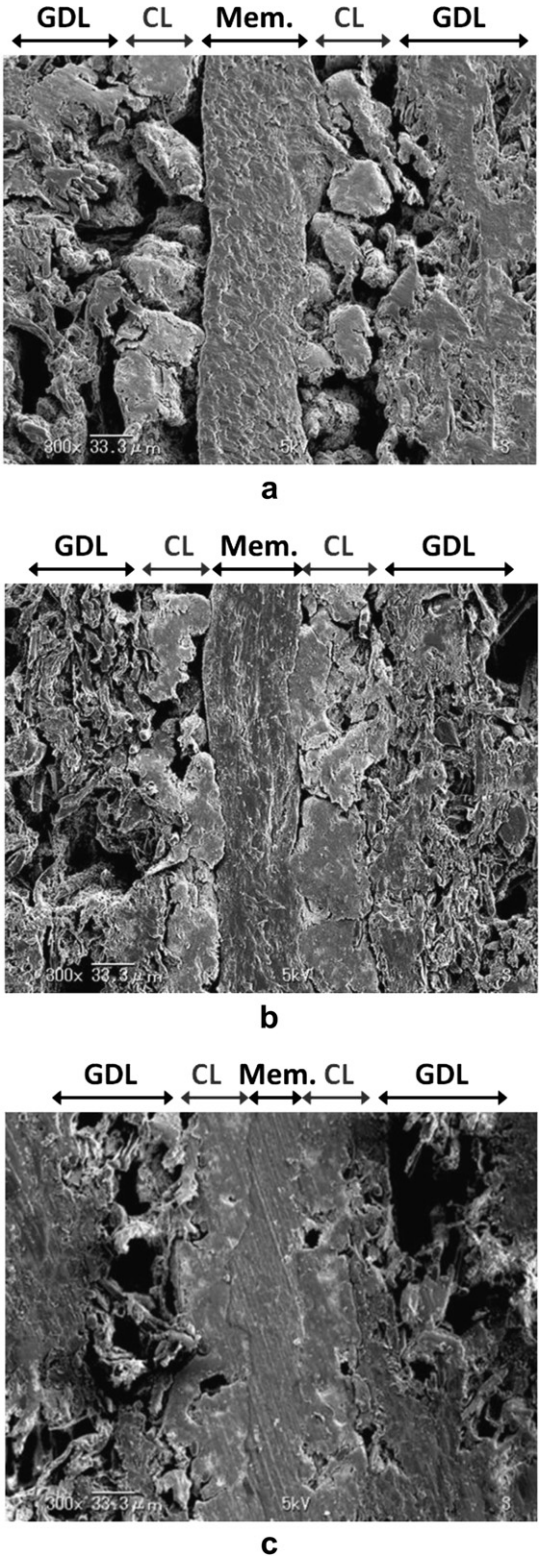

Fig. 6. Cross-sectional SEM images of the MEAs using EMPyr(FH)$_{1.7}$F–HEMA (9:1) composite membrane: (a) before single cell test, (b) after single cell test at 298–353 K, and (c) after single cell test at 393 K. (GDL = gas diffusion layer, CL = catalyst layer, Mem. = membrane.)

298 K to 323 K, single cell performance improves significantly owing to the increase in the electrochemical reaction rate by the elevation of the operating temperature. A maximum power density of 32 mW cm^{-2} is observed at 323 K. However, a small decrease in the power density is observed when the temperature is increased to 353 K. Furthermore, single cell performance is significantly impaired at 393 K.

Fig. 6 shows SEM images of the cross sections of MEAs using the EMPyr(FH)$_{1.7}$F–HEMA (9:1) composite membrane. Before the single cell test, three layers consisting of the membrane, the catalyst layer, and the gas diffusion layer are clearly separated but in good contact with each other. The catalyst Pt/C clusters are also uniformly distributed. However, after the single cell test at 298–353 K, the porosity in the catalyst layer decreases, which restricts the gas transport channels. This deterioration became more obvious for the MEA after the single cell test at 393 K. These results explain the temperature dependence of the single cell performance as follows. At a high temperature, the composite electrolyte in the membrane softens, penetrating into the GDEs and partially plugging the pass in the gas diffusion layer. The deformation of the membrane–electrode layer obstructs the gas supply to the three-phase reaction zone and results in an increase in the mass-transfer resistance. For these reasons, development of a composite membrane that possesses high mechanical strength even at elevated temperatures is necessary.

To improve the single cell performance, optimization of the three-phase reaction zone is necessary. This can be accomplished by the introduction of an ionomer into the catalyst layer. The development of mechanically stronger membranes even at 393 K and the introduction of ionomers are now underway.

4. Conclusions

Composite membranes consisting of EMPyr(FH)$_{1.7}$F and HEMA polymer were prepared and investigated for nonhumidified fuel cells. The composite membranes showed sufficient thermal stability for operation at elevated temperatures up to 423 K. The ionic conductivities of the EMPyr(FH)$_{1.7}$F–HEMA (9:1) composite membrane were 8.7 and 81.9 mS cm^{-2} at 293 K and 393 K, respectively, values that are higher than those for other ionic liquid-based polymer membranes. In the single-cell tests, a maximum power density of 32 mW cm^{-2} was observed at 323 K under nonhumidified conditions. The deterioration of the single cell performance at 353 K is explained by the obstruction of gas flow in GDEs caused by the softening of the composite membrane at elevated temperatures.

Acknowledgments

This work was partly supported by a Grant in Aid for Scientific Research (A) from the Japan Society for the Promotion of Science (JSPS) and the Regional Innovation Creation Research and Development Project from the Ministry of Economy, Trade and Industry of Japan.

References

[1] J. Larminie, A. Dicks, Fuel Cell Systems Explained, second ed., Wiley, 2003.
[2] F. Barbir, PEM Fuel Cells: Theory and Practice, Elsevier Academic Press, New York, 2005.
[3] K.A. Mauritz, R.B. Moore, Chem. Rev. 104 (2004) 4535.
[4] Q.F. Li, H.A. Hjuler, N.J. Bjerrum, Electrochim. Acta 45 (2000) 4219.
[5] C. Yang, P. Costamagna, S. Srinivasan, J. Benziger, A.B. Bocarsly, J. Power Sources 103 (2001) 1.
[6] K.D. Kreuer, S.J. Paddison, E. Spohr, M. Schuster, Chem. Rev. 104 (2004) 4637.
[7] F. Meier, G. Eigenberger, Electrochim. Acta 49 (2004) 1731.
[8] M.A. Hickner, H. Ghassemi, Y.S. Kim, B.R. Einsla, J.E. McGrath, Chem. Rev. 104 (2004) 4587.
[9] I. Gatto, A. Sacca, A. Carbone, R. Pedicini, E. Passalacqua, J. Fuel Cell. Sci. Technol. 3 (3) (2006) 361.
[10] H. Xiuchong, T. Haolin, P. Mu, J. Appl. Polym. Sci. 108 (1) (2008) 529.

[11] J.H. Chang, J.H. Park, G.G. Park, C.S. Kim, O.O. Park, J. Power Sources 124 (1) (2003) 18.
[12] B. Lakshmanan, W. Huang, D. Olmeijer, J.W. Weidner, Electrochem. Solid-State Lett. 6 (12) (2003) A282.
[13] T. Higashihara, K. Matsumoto, M. Ueda, Polymer 50 (23) (2009) 5341.
[14] M. Rikukawa, K. Sanui, J. Prog. Polym. Sci. 25 (2000) 1463.
[15] X. Chen, P. Chen, Z. An, K. Chen, K. Okamoto, J. Power Sources 196 (2011) 1694.
[16] J.S. Wainright, J.-T. Wang, D. Weng, R.F. Savinell, M. Litt, J. Electrochem. Soc. 142 (1995) L121.
[17] J. Lobato, P. Canizares, M.A. Rodrigo, J.J. Linares, G. Manjavacas, J. Membr. Sci. 280 (2006) 351.
[18] D. Plackett, A. Siu, Q. Li, C. Pan, J.O. Jensen, S.F. Nielsen, A.A. Permyakova, N.J. Bjerrum, J. Membr. Sci. 383 (2011) 78.
[19] Y.C. Jin, M. Nishida, W. Kanematsu, T. Hibino, J. Power Sources 196 (2011) 6042.
[20] S. Angioni, P.P. Righetti, E. Quartarone, E. Dilena, P. Mustarelli, A. Magistris, Int. J. Hydrogen Energy 36 (2011) 7174.
[21] S.Y. Lee, A. Ogawa, M. Kanno, H. Nakamoto, T. Yasuda, M. Watanabe, J. Am. Chem. Soc. 132 (28) (2010) 9764.
[22] S.Y. Lee, T. Yasuda, M. Watanabe, J. Power Sources 195 (2010) 5909.
[23] S.S. Sekhon, P. Krishnan, B. Singh, K. Yamada, C.S. Kim, Electrochim. Acta 52 (2006) 1639.
[24] H. Ye, J. Huang, J.J. Xu, N.K.A.C. Kodiweera, J.R.P. Jayakody, S.G. Greenbaum, J. Power Sources 178 (2008) 651.
[25] G. Lakshminarayana, M. Nogami, Solid State Ionics 181 (15–16) (2010) 760.
[26] G. Lakshminarayana, R. Vijayaraghavan, M. Nogami, I.V. Kityk, J. Electrochem. Soc. 158 (4) (2011) B376.
[27] J.T.-W. Wang, S.L.-C. Hsu, J. Electrochim. Acta 56 (7) (2011) 2842.
[28] K.R. Seddon, J. Chem. Technol. Biotechnol. 68 (1997) 351.
[29] T. Welton, Chem. Rev. 99 (1999) 2071.
[30] P. Wasserscheid, W. Kein, Angew. Chem. Int. Ed. 39 (2000) 3772.
[31] R. Hagiwara, Y. Ito, J. Fluorine Chem. 105 (2000) 221.
[32] R. Hagiwara, T. Hirashige, T. Tsuda, Y. Ito, J. Fluorine Chem. 99 (1999) 1.
[33] R. Hagiwara, T. Hirashige, T. Tsuda, Y. Ito, J. Electrochem. Soc. 149 (2002) D1.
[34] R. Hagiwara, K. Matsumoto, Y. Nakamori, T. Tsuda, Y. Ito, H. Matsumoto, K. Momota, J. Electrochem. Soc. 150 (2003) D195.
[35] K. Matsumoto, R. Hagiwara, Y. Ito, Electrochem. Solid-State Lett. 7 (2004) E41.
[36] K. Matsumoto, J. Ohtsuki, R. Hagiwara, S. Matsubara, J. Fluorine Chem. 127 (2006) 1339.
[37] M. Yamagata, S. Konno, K. Matsumoto, R. Hagiwara, Electrochem. Solid-State Lett. 12 (2009) F9.
[38] S. Kanematsu, K. Matsumoto, R. Hagiwara, Electrochem. Commun. 11 (2009) 1312.
[39] R. Hagiwara, Electrochemistry 78 (7) (2010) 626.
[40] T. Enomoto, S. Kanematsu, K. Tsunashima, K. Matsumoto, R. Hagiwara, Phys. Chem. Chem. Phys. 13 (2011) 12536.
[41] R. Hagiwara, T. Nohira, K. Matsumoto, Y. Tamba, J. Electrochem. Solid-State Lett. 8 (4) (2005) A231.
[42] J.S. Lee, T. Nohira, R. Hagiwara, J. Power Sources 171 (2007) 535.
[43] T. Nohira, R. Hagiwara, M. Yamagata, K. Ogasawara, T. Hayashida, in: Abstracts of the 10th Meeting on Materials for Chemical Batteries in Japan, 2008, p. 81.
[44] Y. Tani, T. Nohira, T. Enomoto, K. Matsumoto, R. Hagiwara, J. Electrochim. Acta 56 (2011) 3852.